# Mechanical cleaning of food soil from a solid surface: A tribological perspective

Bistis, Perrakis; Cabedo, Patricia Andreu; Bakalis, Serafim; Groombridge, Michael; Zhang, Zhenyu Jason; Fryer, Peter J.

*DOI:*
10.1016/j.jfoodeng.2023.111858

Journal of Food Engineering 366 (2024) 111858

Contents lists available at ScienceDirect

Journal of Food Engineering

journal homepage: www.elsevier.com/locate/jfoodeng

# Mechanical cleaning of food soil from a solid surface: A tribological perspective

Perrakis Bistis [a,b], Patricia Andreu Cabedo [a,b], Serafim Bakalis [c], Michael Groombridge [b], Zhenyu Jason Zhang [a], Peter J. Fryer [a,*]

[a] School of Chemical Engineering, University of Birmingham, Edgbaston, B15 2TT, UK
[b] Procter & Gamble, Newcastle Innovation Centre, Newcastle-upon-Tyne, NE12 9TS, UK
[c] Department of Food Science, University of Copenhagen, Rolighedsvej 26, Frederiksberg, DK-1958, Denmark

ARTICLE INFO

*Keywords:*
Food foulant
Cleaning rate
Tribology
Mechanical removal
Adhesion
Cohesion

ABSTRACT

In this work, a tribological approach was used to distinguish the synergistic effects of mechanical removal and chemical removal (i.e. dissolution) of a layer of representative food soil from a solid surface, using a tribometer, Mini Traction Machine (MTM). Gravimetric and wear measurements of the soil were used to calculate the cleaning rates of burnt tomato puree on a stainless-steel disc, and the corresponding frictional characteristics offers insight of the mechanical removal. The cleaning due to soil dissolution (chemical removal) was quantified by UV–Vis measurements. The overall cleaning rates of food soil featured a linear reduction in mass over time, with a scaled removal rate $k = 0.0046\ s^{-1}$ (5 N applied force and 100 mm $s^{-1}$ relative velocity), for most cases studied. It was observed that the cleaning rate can be improved with an increasing mechanical load or speed (50% from 1 to 2.5 N and 13% from 50 to 100 mm $s^{-1}$), but is independent of the initial mass. UV–Vis measurements show that by increasing the load or speed the removal of chunks of burnt tomato puree was enhanced more than removal attributed to dissolution. Similar values of cleaning rates for most experimental parameters were extracted from both the gravimetric and wear measurements. Adhesion and cohesion measurements of the burnt tomato puree were conducted with a micromanipulator. It was found that adhesion forces are higher than cohesion for short soaking times, but for longer times the adhesion forces became weaker and with the additional shear rate in the MTM cleaning experiment, adhesion failure was observed in many cases by the end of the experiment. Indentation measurements showed the change in mechanical properties of the food foulant with a few minutes of soaking in water.

## 1. Introduction

Fouling on a solid surface is an undesired accumulation of organic or mineral deposits on the surface (Avila-Sierra et al., 2021a, b; Fryer et al., 2006). A main category of the organic fouling is food deposits. Fouling results from adhesion forces between the deposit and the solid surface as well as cohesion forces of the foulant (deposit). Surface interactions that govern adhesion, the main cause of fouling, include electrostatic forces, van der Waals forces, covalent bond, hydrogen bond. The forces that govern cohesion depend on the chemical nature and microstructure of the fouling material (Liu et al., 2006a; Otto et al., 2016).

A solid surface refers to one that is resistant to penetration of any solid particles and does not absorb liquids, such as stainless steel, kitchen benches, dishes, ceramic tiles, walls, etc. (Uner and Yilmaz, 2015). The removal of the foulant from a solid surface is called cleaning and its main objective is to return the surface to its initial form (Chateau et al., 2004).

Cleaning is a significant everyday life process, hence studying it is crucial. Solid surface cleaning examples include: cleaning of equipment in an industrial process (Vicaria et al., 2017), dish cleaning (Pérez-Mohedano et al., 2017) and in general surface cleaning by wiping or brushing (Uner and Yilmaz, 2015).

Surface cleaning, proposed in recent years by Köhler and colleague, is constituted of four mechanisms: adhesive detachment, cohesive separation, diffusive dissolution, and viscous shifting (Köhler et al., 2019). The action of cleaning could be implemented by either mechanical removal, dissolution in fluid, or chemistry such as surfactants. For solid soils or stains, mechanical removal is the removal of solid soil using

* Corresponding author.
*E-mail address:* p.j.fryer@bham.ac.uk (P.J. Fryer).

https://doi.org/10.1016/j.jfoodeng.2023.111858
Received 15 December 2022; Received in revised form 22 November 2023; Accepted 24 November 2023
Available online 29 November 2023

mechanical force, mainly friction (for solid-solid contact) or liquid shear (for solid-liquid contact). Dissolution of the soil occurs when the liquid phase acts as a cleaning/solvating agent (water or detergent in water). The action of surfactants (detergent) is first the attachment of the hydrophobic part of the surfactant onto the soil and then removal of both surfactants and soil from the surface (Cahn and Lai, 2006). Four actions; wetting of the upper foulant layer, peeling of pieces of the foulant, emulsification of the soil and foaming action (Basso et al., 2017) characterise surfactant cleaning.

The mechanical element of surface cleaning, applying a mechanical forces by a cleaning device (e.g. sponge) directly on a surface foulant, present a different challenge to surface cleaning that was conventionally carried out by fluid only. In here, the applied contact pressure, considering the reduced contact area and enhanced mechanical force, will be significantly greater than that induced by a cleaning fluid. Tribology, the study of friction, wear and lubrication between two interacting surfaces, is thus critical. Friction is the resistance to motion of a solid that is sliding or rolling on another solid in contact with it. Wear is the removal of the material or damage that is caused to a solid during friction. Lubrication occurs when there is a fluid between the two surfaces, which decreases the friction and as a result reduces wear (Bhushan, 2013; Blau, 2009). During a cleaning process of a food deposit from a solid substrate, friction is the main force that is applied from the cleaning device on the food foulant, removal of solid particles from the food deposit is the wear and cleaning liquid can lubricate the process. Thus an equipment that can measure the horizontal (frictional) force and provide the friction coefficient, which is the horizontal divided by the vertical force and study the lubrication and wear of the system can be a powerful tool to study solid surface cleaning of food deposits (Prakash, 2017). Unlike the cleaning action applied by liquid whereby a uniform shear stress is imposed across the sample surface by the flow, stress on the normal direction is limited to the area of contact in mechanical cleaning. Another critical parameter is the swelling kinetics of the soil upon exposure to cleaning fluid, which changes its physical properties such as cohesiveness considerably (Joppa et al., 2017, 2019, 2020).

Liu et al. (2002) developed a micromanipulation probe to measure the horizontal force to remove the soil completely, but the normal force was not measured. There are a few tribology analyses of cleaning processes in the literature. Mercadé-Prieto and Bakalis (2013, 2014) focused on fabric cleaning, measuring cotton-cotton abrasion in a tribometer and a washing simulator rig. They concluded that abrasion is not very effective in cleaning model soils, but can reduce fat content from the fabrics. Lütkenhaus et al. (2016) studied protein-based soil removal from stainless steel in a tribometer and showed that increasing the normal load on the protein soil decreased the friction or traction coefficient. These studies used the Mini Traction Machine (MTM), which provides a chamber with controlled environment into which liquid can be added, the applied vertical force can be controlled and the frictional force measured. The MTM has been widely used for purposes such as understanding oral processing of food (Taylor and Mills, 2020), and investigating the influence of co-solutes of agar fluid gels on tribology (Fernández Farrés and Norton, 2015).

The aim of this study was to evaluate simultaneously the tribological properties and the cleaning rate of the removal of a food deposit from a solid surface. For that purpose, a tribometer (MTM) was used. Burnt tomato puree on stainless steel was selected as a representative food soil. The change of physical properties of this soil as a function of time in the water was measured both by indentation and micromanipulation methods. The experiments simulate the practical situation of removing a food deposit when a mechanical force is applied. Cleaning rates were calculated both gravimetrically and by the wear values and gave similar results. The effect of different parameters on cleaning rate was investigated and showed increased cleaning rate for increasing normal load and speed and no effect for different soil mass. By using UV–Vis, two main cleaning mechanisms were identified, dissolution and chunk removal.

## 2. Experimental

### 2.1. Materials

Tomato purée was purchased from a local supermarket, the composition of which per 100 g includes carbohydrate 17.1 g (sugars 13.6 g), protein 4.4 g, fat 0.5 g, fibre 2.6 g, salt 0.38 g, and water 75 g. Tap water was used (20 °C) as liquid media in the MTM to replicate a household cleaning process. Stainless steel (AISI 440C grade) discs (46 mm diameter, 4 mm annulus width, $R_a < 0.05$ μm) and balls (3/4 inch diameter) were purchased from PCS Instruments (UK), cleaned in isopropanol, followed by distilled water, in an ultrasound cleaner for 6 min prior to each experiment (Taylor and Mills, 2020).

### 2.2. Sample preparation

Tomato purée was placed on the stainless-steel disc, which in turn was placed in the oven (110 °C, 1 h) to form a burnt-on deposit. Fig. 1 shows the three stages of the preparation, where the weight of the disc was measured for each case (resolution: 0.001 g). These conditions produced a deposit soil on the stainless steel that was difficult to remove. Typical mass was ~58.5 g for the discs and an additional 0.5 ± 0.05 g for the burnt tomato puree.

### 2.3. Mini Traction Machine

The MTM is a tribometer that measures the frictional properties of lubricated and unlubricated contacts. As shown in Fig. 2, it consists of a rotating ball in contact with a rotating disc in a chamber. The chamber can be either open, to observe the experiment, or closed to control the temperature.

For the cleaning and tribology experiments, a Mini Traction Machine (MTM) tribometer (MTM2, PCS Instruments, London) was used. Parameters that can be controlled are temperature ($T$), applied load ($F_L$), entrainment speed (U) that is the mean of the ball and the disc speed, and the slide roll ratio (SRR) defined as:

$$\mathrm{SRR} = \frac{U_{\mathrm{disc}} - U_{\mathrm{ball}}}{U} \tag{1}$$

The frictional force, $F_f$, applied on the ball is measured by a force transducer and the traction or friction coefficient ($\mu$) is calculated according to its definition:

$$\mu = \frac{F_f}{F_L} \tag{2}$$

In addition other sensors can measure wear, by on-line wear measurements that detects the height of the ball and temperature (Garrec and Norton, 2012).

### 2.4. Hydration and UV–vis spectroscopy calibration curve

The action of water penetration, resulting in the dissolution of the burnt tomato purée, was quantitatively measured by a UV–Vis

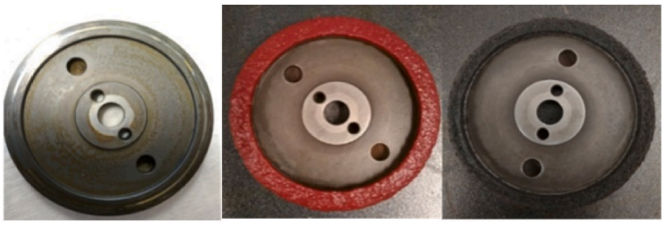

**Fig. 1.** Sample preparation of representative food soil, a: a plain MTM disc, b: fresh tomato purée placed on measurement area of the MTM disc, and c: burnt tomato purée after the thermal treatment.

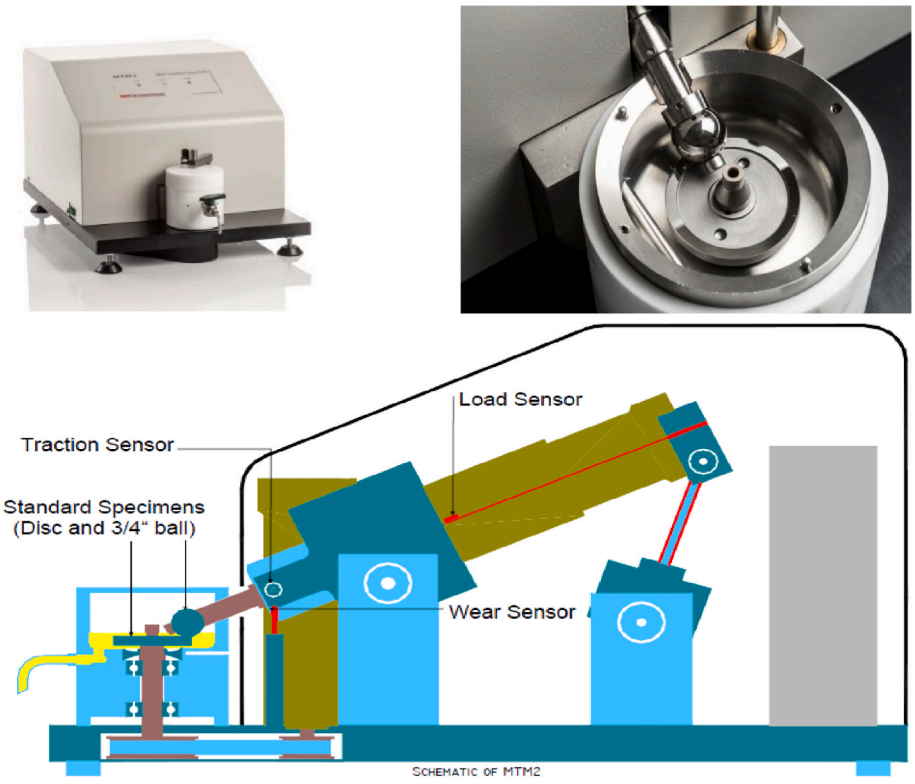


**Fig. 2.** Mini Traction Machine apparatus. (top left): Picture of the instrument, (top right): Picture of the chamber where the experiment is happening, (bottom): Schematic of main parts of the apparatus (“MTM (Mini Traction Machine) | Products | PCS Instruments,” 2017).

spectrometer (Biochrom Libra S12 apparatus). Different MTM discs with burnt tomato purée, prepared by the thermal method above, were placed in a petri-dish with 60 mL of tap water at 20 °C, for different exposure time (1 s, 30 s, 1 min, 2 min, 5 min, 10 min, and 20 min). The discs were subsequently placed in an oven (60 °C, 24 h) to remove the residual water. The difference in the measured mass of the deposit provides a quantitative indication of chemical removal under static condition. The liquid in every petri-dish was stirred with a magnetic stirrer to produce a homogenous suspension, from which 1 mL was sampled for the UV–Vis calibration curve. For the UV–Vis measurements the wavelength used was $\lambda = 470$ nm, where lycopene in tomato shows a peak (Bunghez et al., 2011).

### 2.5. Cleaning experiment in Mini Traction Machine (MTM)

After sample preparation, the MTM discs, with the burnt tomato puree, were placed in the MTM chamber. Measurements were made as a function of the applied load (between 1 and 5 N) that is the ordinary range a human would apply during mechanical cleaning, the mass of the burnt tomato puree (0.3 and 0.5 g), and the entrainment speed (from 50 to 200 mm $s^{-1}$), of which the parameters are summarised in Table 1. The SRR chosen was 50% based on preliminary test results. Each experimental condition was repeated three times to ensure reproducibility.

**Table 1**
MTM different experimental parameters (*different sample/experiment for every 0.5 min, **different sample/experiment for every 1 min).

| Types of experiment | Mass (g) | Load (N) | Speed (mm $s^{-1}$) | Time (min) |
|---|---|---|---|---|
| Main parameters | 0.5 | 5 | 100 | 3* |
| Mass factor | 0.3 | 5 | 100 | 2* |
| Load factor 1 | 0.5 | 2.5 | 100 | 3* |
| Load factor 2 | 0.5 | 1 | 100 | 5** |
| Speed factor 1 | 0.5 | 5 | 200 | 3* |
| Speed factor 2 | 0.5 | 5 | 50 | 3* |

Experimental duration was 2,3 or 5 min (Table 1) depending on the cleaning efficiency and then the disc was withdrawn from the MTM chamber.

After the disc was placed in the MTM chamber, 60 mL of water were added (20 °C). The MTM took an average of 30 s from the start command to the beginning of the measurement, thus no readings could be taken until 30 s of cleaning had elapsed. During the experiment, the traction coefficient was measured continuously. At the end of the experiment a liquid sample was taken with a syringe filter to identify the concentration of the dissolved tomato puree in the liquid, by UV–Vis measurements, using the calibration curve extracted from the hydration experiments. Then the disc was removed from the machine and placed in the oven (60 °C, 24 h) to remove the water so that the remaining mass of tomato puree could be measured accurately. 60 °C was chosen because at higher temperatures both water and other volatiles were lost, and to avoid Maillard reactions that changed the composition of the soil (Maillard, 1912). By this method, both the weight of puree removed and the liquid concentration were determined.

### 2.6. Micromanipulation measurements

#### 2.6.1. Cohesion and adhesion measurement

A custom-built micromanipulation device was used to measure adhesion and cohesion forces of surface foulant; full experimental details are described in previous studies (Herrera-Márquez et al., 2020; Liu et al., 2002). The main parts of the equipment are a stainless-steel scraper (25 mm scraping size) attached to a force transducer (Sauter, model: FH 5) with capacity of 5 N. The equipment has a moving base with 5 chambers to place the coupons. During the experiment the scraper is placed in front of the sample and the chamber moves so that the scraper removes the sample from the coupon. The force applied on the scraper is measured and the adhesive or cohesive strength is calculated by the following equations (Herrera-Márquez et al., 2020; Liu et al., 2002):

$$W = \frac{d}{t_C - t_A}\int_{t_A}^{t_C} F dt \tag{3}$$

$$\sigma = \frac{W}{\alpha A} \tag{4}$$

where $W$ is the work of the force applied on the transducer, $d$ is the length of the sample being removed, $t_A$, $t_C$ are the initial and final time when the scraper was removed from the sample, $F$ is the force applied on the scraper, $\alpha$ is the ratio between surface area of the tomato and the surface area of the coupon, $A$ is the surface of the coupon, and finally $\sigma$ is the adhesion/cohesion strength.

Sample preparation was similar to the MTM experiments, but the tomato puree was placed on square coupons instead of the MTM discs. The samples with the burnt tomato puree were placed in the micromanipulator with 10 mL of water for soaking purposes. Adhesion and cohesion measurements were taken by changing the scraping height, so material was fully removed from the surface (adhesion) or the deposit but cut to leave material on the surface (cohesion measurement). For adhesion that height was ~100 μm, which was a safe distance from the surface that would fully remove the material and for cohesion the cut height was ~300 μm. The probe height was adjusted with a use of a microscope camera (Kranich ×1000 magnification, 2 MP).

#### 2.6.2. Indentation

Indentation experiments were conducted using the micromanipulation rig in a vertical position, demonstrated in previous studies by Oliver and Pharr (1992, 2004). These experiments measured the Young's modulus of burnt tomato puree to facilitate the estimation of the approximate applied pressure of the stainless-steel ball on the soil, in the MTM cleaning experiments, assuming a Hertzian contact (Borodich and Keer, 2004; Hertz, 1882). The specimen used for the indentation was a stainless-steel cone with an angle of 50°, 8 mm height (Arzate-Vázquez et al. (2015)). The indentation speed and depth were kept at 0.02 mm $s^{-1}$ and 0.8 mm respectively, and soaking time was varied (2, 3, 4 and 10 min) before indentation was carried out. The equations used for calculating the contact pressure were:

$$S = \left(\frac{dL}{dh}\right)_{h=h_{max}} \tag{5}$$

$$h_c = h_{max} - \varepsilon\frac{L_{max}}{S} \tag{6}$$

$$A = \left[(h)_c \tan\theta\right] \tag{7}$$

$$E = \frac{\sqrt{\pi}}{2\beta}\frac{S}{\sqrt{A}} \tag{8}$$

where $S$ is the contact stiffness, corresponding to the slope of the upper portion of the unloading curve (Fig. 3) during the initial stages of unloading; $L$ is the load, $h$ is the displacement, $h_c$ is the estimated contact depth (difference between the maximum displacement, $h_{max}$ and the sink in of the sample, which is defined by the second part of Eq. (6), and represented by the displacement of the soil due to indentation (Oliver and Pharr, 2004)), $\varepsilon$ is a constant determined by the geometry ($\varepsilon = 0.72$ for conical indenter), $A$ is the projected contact area, $\theta$ is the indenter angle (50°), $E$ is the reduced elastic modulus for the sample and indenter, $\beta$ is a dimensionless parameter used to eliminate for deviations in stiffness due to lack of axial symmetry for pyramidal indenters (in this case β = 1.05 (Fischer-Cripps, 2011)).

Once the modulus has been measured, the MTM data was interpreted by Eqs. (9) and (10), whereby $F$ is the applied force, $A_r$ is the real contact area of the stainless steel ball on the burnt tomato puree in the MTM, $R$ the radius of the ball and $P$ the actual contact pressure (Arzate-Vázquez et al., 2015; Garrec and Norton, 2012; Hertz, 1882; Oliver and Pharr, 2004).

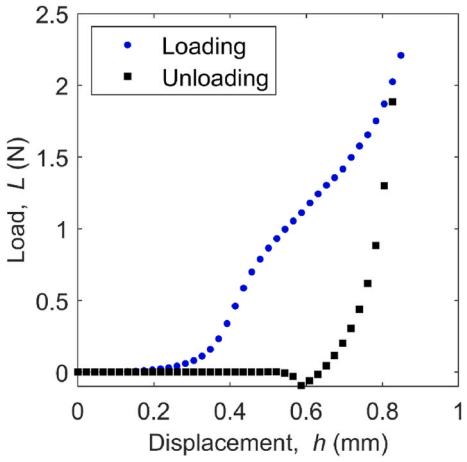


**Fig. 3.** A representative indentation plot of burnt tomato puree sample being immersed in water for 4 min. It includes a loading curve (blue), where the load is increased and an unloading curve (red), where the load is decreasing. Contact between indenter and soil sample was made when the load started to increase. The main quantities to be measured are the maximum load $L_{max}$, the maximum displacement $h_{max}$, and the stiffness $S$ was calculated by Eq. (5).

$$A_r = \pi\left(\frac{3FR}{4E}\right)^{\frac{2}{3}} \tag{9}$$

$$P = \left(\frac{F}{A_r}\right) \tag{10}$$

### 2.7. Statistical analysis

All graphs represent the averaged values of at least three independent measurements, of which the standard error values are used as the error bars.

## 3. Results and discussion

### 3.1. Physical properties of tomato puree

#### 3.1.1. Young's modulus of burnt tomato puree

At first, indentation experiments were performed on the burnt tomato puree sample to determine its Young's modulus, which was subsequently used to calculate the contact pressure during the cleaning experiment (Oliver and Pharr, 1992, 2004). A representative indentation graph (force *vs* displacement plot) is shown in Fig. 3, whereby both approaching (blue) and retraction (red) processes are included. Different soaking times were investigated to make sure that suitable and correct applied pressure values were used for interpreting the MTM data during the cleaning process. Fig. 4 shows the pressure applied by the stainless-steel ball on the burnt tomato puree for three different loading forces and two soaking times, corresponding to the start and end points for a typical cleaning experiment. During such time the applied pressure was reduced by nearly 20%, which is attributed to the hydration upon exposure to water. Experiments with soaking times between 2 and 10 min were attempted, all of which showed similar applied pressure values. The Young's modulus of the burnt tomato puree was estimated to be ~30 MPa for the few seconds of soaking and ~21 MPa after 2 min soaking. The values of Young's modulus are in the same order of magnitude reported on chick-pea roots (Kurowski et al., 2018) and potato (Sinha and Bhargav, 2020), which are up to 300 MPa and approximately 3 MPa, respectively.

#### 3.1.2. Cohesion and adhesion of burnt tomato puree

Cohesion force of the burnt tomato puree samples and their adhesion

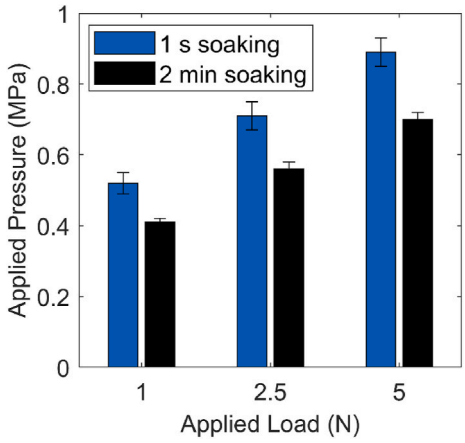


**Fig. 4.** Pressure of the ball applied on the burnt tomato puree for 1 s and 2 min soaking, under three loading forces.

force to the supporting stainless-steel substrates, measured by the custom-built micromanipulation rig, are presented in Fig. 5. For samples with a soaking time less than 15 min, foulant removal was observed in limited regions, which corresponds to a cohesion energy of 80–100 J $m^{-2}$, whilst adhesion energy was beyond the measurement limit of the instrument (5 N, corresponding to a cohesive energy of >200 J $m^{-2}$). After 20 min of soaking, complete removal of burnt tomato puree was observed in certain regions of the contact area, and the adhesion energy (40 J $m^{-2}$) was ~22% less than the cohesion energy (51 J $m^{-2}$). This suggests that water molecules could diffuse into the burnt tomato puree, and weaken the intermolecular interactions between the denatured proteins, but also penetrate to the interface of foulant and stainless steel, reducing the adhesion forces. Finally, for prolonged soaking times (≥25 min), complete removal was found over a good fraction of the fouled area, evidencing that the adhesion energy is considerably less than cohesion energy: after 25 min of soaking the cohesion forces were higher (18 J $m^{-2}$ adhesive strength and 26 J $m^{-2}$ cohesive strength); after 30 min of soaking time, no complete cohesion measurements could be made as some of the soil was completely removed from the surface at all measurements with a probe height designed to identify cohesion; finally, at 40 min, only adhesive removal was observed for both probe heights with very low strength (1 J $m^{-2}$).

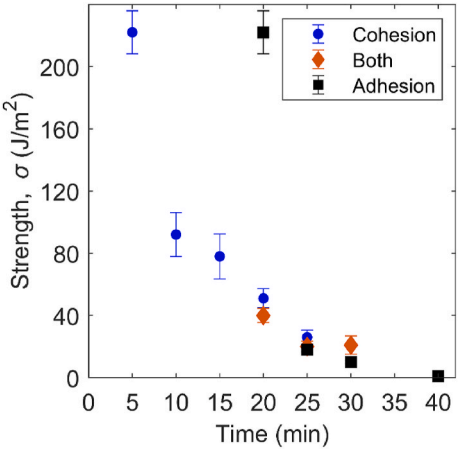


**Fig. 5.** Cohesion (soil – soil interaction) and adhesion (soil – surface interaction) strength or both cohesion and adhesion observed, of burnt tomato puree samples as a function of immersion time in water. In the case of cohesion, a layer of tomato puree is removed leaving another layer on the coupon, for adhesion the whole tomato puree is removed from the coupon and for both cohesion and adhesion a percentage of the surface is clean.

Values of measured adhesion and cohesion, as a function of the immersion time, are summarised in Fig. 5. Our results indicate that the adhesion between burnt tomato puree and stainless steel is greater than the cohesion in the initial stage (20 min), as the adhesion energy was beyond the measurement upper limit. Upon exposure to water, diffusion of water molecules into the matrix of denatured proteins and penetration of water to the tomato-stainless steel interface, which causes soil swelling and weakens both cohesion energy and adhesion energy, respectively (Hooper et al., 2006; Liu et al., 2002, 2006b). The nature and magnitude of the interfacial interaction is largely determined by both characteristics of the food soil and the solid substrate in contact. As a result, the measurement of that weakening of the mechanical strength (cohesion/adhesion) is possible by the micromanipulator and indentation, as a function of exposure time and indentation depth. However, the rate of adhesion weakening (40.8 N $min^{-1}$ assuming that adhesion at 20 min is the lowest value that cannot be measured) is considerably greater than that of cohesion weakening (26.0 N $min^{-1}$), evidenced by the arbitrary gradients introduced to the values, which is likely due to the hydrophilic nature of stainless steel, offering favoured interaction with water molecules where possible. The rate of adhesion/cohesion weakening could be an invaluable indicator for cleaning tough soils, as it can be controlled not only by immersion time, but temperature, soil, substrate, and cleaning technologies used. It is worth noting that the assumption made here is that the rate of reduction at the early hydration stages, follows a linear fashion, which is unlikely to be perfectly accurate, and warrants future investigation.

This decrease in cohesion strength throughout the experiment should be a product of swelling of the soil due to the absorption of water. The further penetration of water in the puree - stainless steel interface causes adhesion strength to weaken with time as displayed in Fig. 5.

In a previous study by Liu et al. (2002) both cohesion and adhesion energy of a commercial tomato paste were measured with a micromanipulation rig. A similar trend was reported, in that cohesion energy was greater than adhesion after a soaking time that made measurements possible, but in our work a shifted balance between cohesion and adhesion over time was observed. Also the values in Liu et al. (2002) were much lower (for 25 min soaking the partial removal was ~4 J $m^{-2}$ and the total removal was ~2 J $m^{-2}$), compared to the tomato puree of this study. This difference could be due to be the composition of the tomato products, the type and roughness of stainless-steel solid surface, the sample preparation method or different conditions which led to such higher adhesion and cohesion forces for similar baking and soaking times.

### 3.2. Tribology and cleaning

#### 3.2.1. Hydration and cleaning rates

Building upon the effect of water on both cohesion and adhesion of surface foulant, MTM measurements were carried out to differentiate the contribution of cleaning solution versus mechanical force applied by capturing both tribological characteristics and cleaning profiles simultaneously, when moving the stainless-steel ball against the burnt tomato puree samples laterally.

Here, $R_M$ is used to quantify the relative mass of surface foulant at a given time, as shown in Eq. (11). The relative mass was used to eliminate any mass differences between samples. This relative mass format was not used only when the effect of deposit mass was being studied directly.

$$R_M(t) = \frac{m(t)}{m_o} = \frac{tomato\ mass\ at\ t = \mathrm{t}}{tomato\ mass\ at\ t = 0} \tag{11}$$

Fig. 6 presents the relative mass over time, with and without mechanical force applied. The benchmark, with no mechanical input, was acquired by placing a prepared burnt tomato puree sample in water under static condition. The benchmark shows that approximately 20% of the initial mass was removed over 300 s, as the result of dissolution. In contrast, complete removal was accomplished within 200 s when 5 N

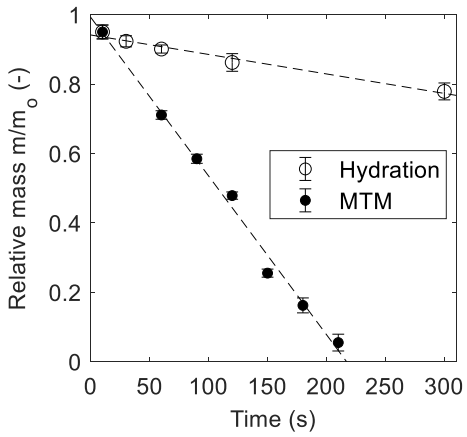


**Fig. 6.** Hydration vs MTM experiment. This figure shows the relative mass, $R_M$, of burnt tomato puree during a hydration-only experiment (where the disc was placed in water and the mass loss was measured over time) and a cleaning experiment in MTM under water with applied load of 5 N, speed of 100 mm $s^{-1}$ and initial soil mass of 0.5 g.

force was applied. The slope for both datasets appear to be linear, suggesting that the removal process follows zero order kinetics, i. e the cleaning takes place at a constant rate. Eq. (12) was subsequently used to describe the cleaning efficiency:

$$\frac{1}{m_o}\frac{dm(t)}{dt} = -k \tag{12}$$

where $k$ is cleaning efficiency or cleaning rate. The cleaning efficiency for the hydration experiment was 0.0006 $s^{-1}$ and for the MTM cleaning experiment was 0.0046 $s^{-1}$. This indicates that the additional load and shear rate in the MTM chamber accelerate the process 7 to 8 times. It is worth noting that the removal rate does not follow a linear relationship in the hydration condition (no mechanical removal involved), whereby the removal rate in the first 10 s was significantly greater than that for the rest of the measurements.

### 3.2.2. Correlation between tribology and cleaning

MTM measures the traction (friction) coefficient between a stainless steel ball and the surface foulant during the cleaning process: a representative set of friction coefficient data over time is shown in Fig. 7 to demonstrate the evolving nature of the interfacial interaction, controlled by the hydration process of the soil and the mechanical force applied.

Initially, the traction coefficient was high due to the surface roughness of the prepared burnt tomato puree. It decreases over the first 20 s (blue region), which is likely the result of a synergistic effect of soil hydration and mechanical removal. At the end of this phase, the sample surface was found to become smooth, but covered the MTM disc uniformly without any visible rupture. The traction coefficient remained constant (Fig. 7 left, picture b area), with a constant cleaning efficiency, which suggests that the removal is due to cohesion failure. Visual inspection shows that a few regions of the burnt tomato puree were removed, exposing the stainless-steel disc underneath. A steadily increased traction coefficient was subsequently observed (green region), during which the majority of the soil was removed, indicating that the removal is due to adhesion failure. The traction coefficient continued to increase (black region), now corresponding primarily to friction between the stainless-steel disc and the counter ball, with negligible contribution from the remaining soil. In the final phase, the traction coefficient became steady, with all deposit removed and sole remaining contact between the stainless-steel ball and disc.

Although the overall duration of the micromanipulation experiments is greater than that of MTM measurements, the adhesion and cohesion data is valuable in understanding the removal mechanism of burnt tomato puree samples. Initially, adhesion between tomato deposit and the stainless-steel underneath is substantially greater than cohesion, which limits the removal to being from the soil surface, and thus the removal amount. It is very likely that the mechanical load applied on the normal direction, and the corresponding friction force, could remove the food soil in a continuous manner, which exposes the soil buried underneath to water. This mechanical action would accelerate the penetration of water molecules into the matrix of soil, which weakens both cohesion and adhesion, resulting in an increased soil removal. It is worth noting that the specific cleaning mechanism, whether it is due to adhesive or cohesive failure, is determined by the nature of the soil, magnitude of the adhesion/cohesion, and the kinetics involved.

### 3.2.3. Effect of cleaning parameters

Measurements were carried out to investigate the effects of parameters such as soil thickness, applied load, and velocity on cleaning performance. Fig. 8a shows the tribological characteristics and cleaning profiles of samples with two different weights (0.3 and 0.5 g) of burnt tomato puree, showing that identical features were observed. First of all, the reduction in relative mass follows zero order kinetics, and the cleaning rate (slope of the relative mass), $k' = k \bullet m_o$, equals 0.0024 g $s^{-1}$ in both studies. This suggests that the cleaning rate is independent of the soil thickness, supporting the proposed explanation that the primary cleaning mechanism is due to cohesion failure at the surface of the soil. The traction coefficient was found to start with similar values, and

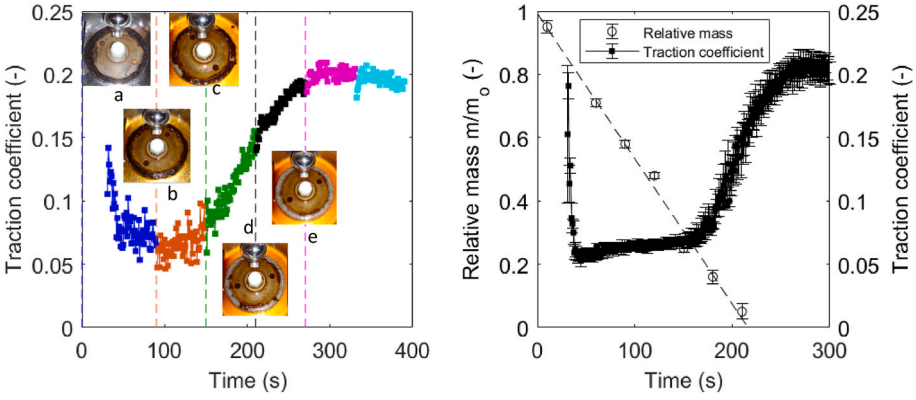


**Fig. 7.** (A) Graph of traction coefficient vs time in the MTM (load 5 N, speed 100 mm $s^{-1}$, SRR 50%, T = 20 °C, $m_o$ = 0.5 g). Picture a: MTM disc with the burnt tomato puree in the MTM chamber before the experiment. Picture b: Same disc after 90 s of experiment. Picture c: After 150 s. Picture d: After 210 s. Picture e: After 270 s. (B) Comparison of the traction coefficient data with the relative mass during the cleaning experiment (a typical graph with applied load 5 N, speed 100 mm $s^{-1}$ and 0.5 g mass).

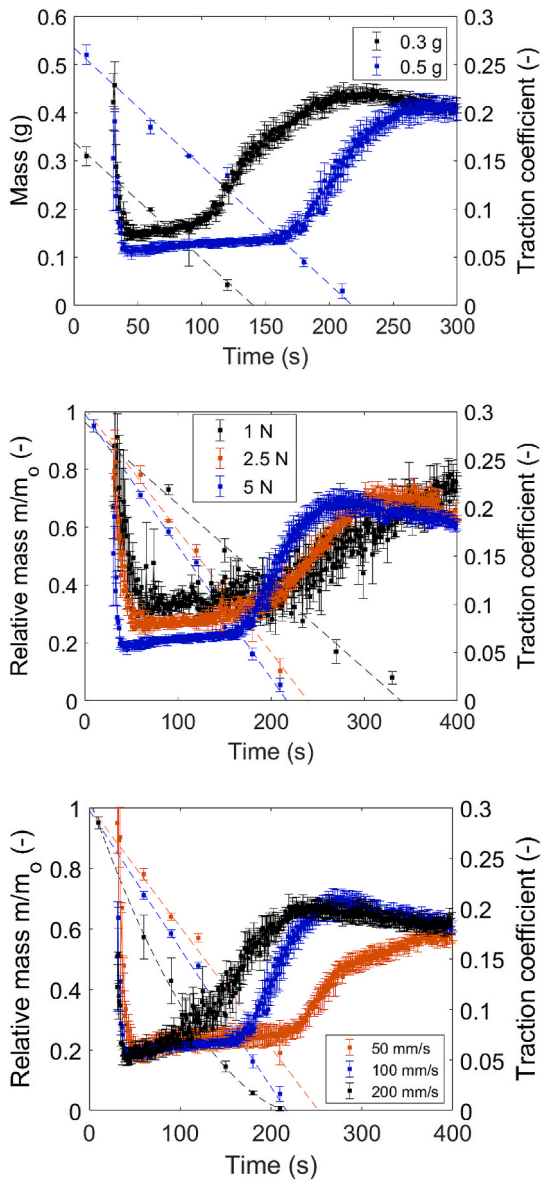


**Fig. 8.** Cleaning rate and traction coefficient diagrams for different conditions (initial mass, load and speed). (Top): Mass & Traction coefficient vs time comparing 0.3 g and 0.5 g of burnt tomato puree. (Middle): Mass & Traction coefficient vs time comparing 1, 2.5 and 5 N applied load. (Bottom): Mass & Traction coefficient vs time comparing 50, 100, 200 mm $s^{-1}$ speed.

subsequently reached a plateau after nearly an identical time span (~10 s), which confirms our rationale that this is an effectively 'smoothing' process of the soil surface. The only difference is that the increase in traction coefficient took place sooner for the 0.3 g sample than the 0.5 g one (at ~100 s rather than ~170 s). This is because the soil removal is due to surface cohesive failure, and hence less time is required to clean a thinner soil, whilst the traction coefficient was constant during this process. In all experiments, it was observed that the traction coefficient started to increase when chunks of tomato puree were removed, exposing the stainless-steel surface, which suggests an adhesion failure.

The effect of the force applied on the normal direction is presented in Fig. 8b, where three loading forces, 1, 2.5 and 5 N, are compared. The surface smoothing process, as reflected by the decreased traction coefficient in the very initial phase, appears to be controlled by the applied load – the higher the load, the sooner it takes to reach the plateau. Likewise, the cleaning rate follows zero order kinetics as observed in other measurement and is determined by the applied load – $k$ equals to 0.0046, 0.0042, and 0.0028 $s^{-1}$ for 5, 2.5, and 1 N, respectively. The transition point from plateau to the increasing slope, used to determine the completion point of cohesion failure, is also correlated with the applied load. It takes less time to remove the same amount of soil when a greater loading force is applied, which is consistent with the cleaning efficiency result.

The difference between 1 and 2.5 N is clearly bigger than 2.5 and 5 N. This was also visible during the experiments, since more chunks of tomato puree were removed at 2.5 and 5 N rather than 1 N. This can be seen also from the absorbance graphs (Fig. 10) where the dissolved tomato puree % is much higher than the chunk removal in the case of 1 N.

Fig. 8c shows that an increased speed, or shear rate, could result in an improved cleaning rate. For 50 and 100 mm $s^{-1}$ cleaning velocity, the data shows a linear decrease with time, as observed in all cases presented so far. However, for cleaning velocity of 200 mm $s^{-1}$, the relative mass graph shows a non-linear characteristics, which is likely the result of the removal of large pieces of deposit from the substrate during the early stage of the experiment (~ first 100 s), forming cleaned areas of stainless steel. The ball is only in contact with the fouled part of the disc for a fraction of the time during the experiment, which extends the total cleaning time measured. That was the case for all experiments when a part of the stainless-steel disc was revealed, but was happening later for all other experiments, which leads to the difference being negligible thus does not change the cleaning rate behaviour. The traction coefficient starts increasing earlier for the fastest cleaning (200 mm $s^{-1}$) since the ball is in contact with the disc faster than the slower experiments. The chunks of tomato puree removed in the 200 mm $s^{-1}$ case were significantly bigger than all other cases and that can be seen in Fig. 10 and will be discussed later.

### 3.2.4. Correlation between removal mass and wear

The vertical position of the ball was monitored during the cleaning experiment by MTM, which offers an insightful correlation between wear kinetics and cleaning. The wear is given by the vertical position change of the MTM ball during the experiment, which means that the soil that was in a higher position earlier in the experiment has been removed or worn. Fig. 9 compares the relative mass reduction of the 2.5 N experiments (2.5 N, 100 mm $s^{-1}$, 0.5 g) with the corresponding relative wear change that is defined by the following equation:

$$R_W(t) = \frac{w(t)}{w_o} = \frac{tomato\ average\ thickness\ at\ t = t_1}{tomato\ average\ thickness\ at\ t = 0} \quad (13)$$

The wear against time graph shows a linear behaviour similar to mass against time. This suggests that the mass loss and the decreasing sample thickness or wear may have similar rate behaviour. To identify any correlation, it was assumed that the thickness of the sample was ~5% smaller after 10 s of soaking, using the value from the hydration graph, Fig. 6. This assumption was necessary, to estimate the average initial thickness, $w_o$, of the burnt tomato puree sample. The average thickness for each sample was used, since the tomato puree thickness varies around the disc, as found by the wear measurements (~100 μm variation for thicknesses ~1000 μm). The initial mean thickness of the sample was back calculated by the trend-line of wear against time graph, where it was assumed that the thickness will be the 95% of the initial thickness at 10 s of the experiment. The wear vs time graph (Fig. 9a) though gave an unsatisfying trendline ($R^2 < 0.90$) due to sample thickness variability, which can become larger after a hole in the tomato ring is created. To eliminate this error the average value for each wear value was extracted, w(t) (the average of 11 wear values, −5 and +5 s of the original value (1 measurement/s), ~11-disc rotations). That mean initial thickness, $w_o$, was used to divide the average wear measurements, w(t), (Eq. (13)) and produce the relative wear graph (Fig. 9 right). In the case of Fig. 9 the slopes, or cleaning rates were calculated as equal and the graphs look similar.

Table 2 compares the rate constants of the relative mass against time (Eq. (12)) and relative wear against time graphs:

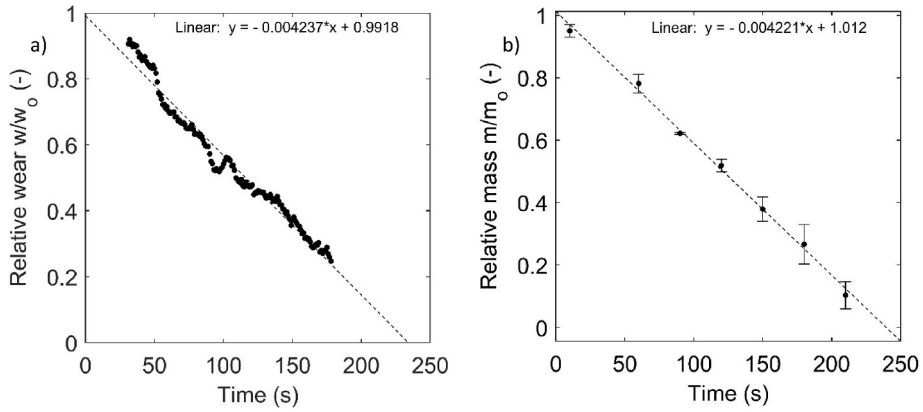


**Fig. 9.** Comparison of relative wear (a) with relative mass (b) graphs. Conditions: 2.5 N, 100 mm s$^{-1}$, 0.5 g with 3 repeats.

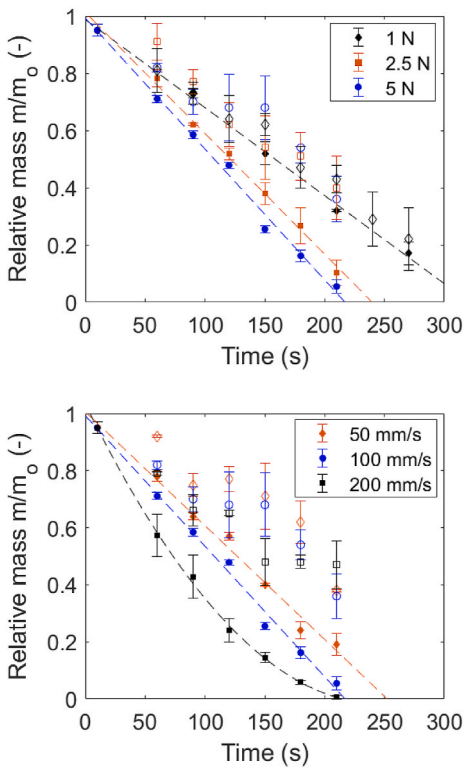


**Fig. 10.** Total removed relative mass (•) vs removed relative mass due to dissolution (o). The lines represent the trendlines for the total removed relative mass. (Top) Load variation (Bottom) Speed variation. The rest of the values for each case can be found in Table 1.

**Table 2**
Comparison of cleaning rates extracted from the wear measurements and mass measurements. The universal conditions are 5 N, 100 mm s$^{-1}$, 0.5 g.

| Characteristic Conditions | Cleaning efficiency Wear $\frac{\mu m}{\mu m \cdot s}$ | Cleaning efficiency Mass $\frac{g}{g \cdot s}$ |
|---|---|---|
| 1 N, 100 mm s$^{-1}$, 0.5 g | −0.0031 ± 0.0002 | −0.0028 ± 0.0003 |
| 2.5 N, 100 mm s$^{-1}$, 0.5 g | −0.0042 ± 0.0002 | −0.0042 ± 0.0003 |
| 5 N, 100 mm s$^{-1}$, 0.5 g | −0.0048 ± 0.0001 | −0.0046 ± 0.0002 |
| 5 N, 50 mm s$^{-1}$, 0.5 g | −0.0043 ± 0.0001 | −0.0040 ± 0.0002 |
| 5 N, 100 mm s$^{-1}$, 0.3 g | −0.0071 ± 0.0003 | −0.0066 ± 0.0006 |

$$\frac{1}{w_o}\frac{dw(t)}{dt} = -k \tag{14}$$

In general, the values are similar, which suggests that wear measurements can be used to evaluate cleaning rates for this experiment. The biggest difference was found in the case of 0.3 g. The main reason for this was probably the fact that in this experiment the tomato puree was removed in the shortest time. This caused earlier adhesive removal that lead to contact of the stainless-steel ball and disc for a longer time, thus there was less contact between the stainless steel ball and the burnt tomato puree. In addition, the wear values for 200 mm s$^{-1}$ experiment did not correlate with the mass results, probably because of the same reason.

### 3.2.5. *Cleaning mechanisms and measured absorbance*

In the MTM experiments, where water is used as a cleaning liquid, two main cleaning mechanisms were observed: dissolution and mechanical removal. Liquid suspensions were acquired from the MTM chamber for UV–Vis measurements to quantify the dissolution mechanism of the cleaning.

Fig. 10 compares relative mass reduction graphs (Figs. 8a, 7c and 7e)) measured by removing discs from the MTM and weighing directly, with the relative dissolved mass obtained by using the calibration curve (y = 0.00427 x) to establish the dissolved mass, which was then divided by the initial deposit mass. Fig. 10 shows that by increasing the load or speed, mechanical removal was enhanced, since the difference between the removal due to dissolution (Fig. 10: empty dots) and the total removal (Fig. 10: full dots), is greater. In case of load increase this was expected, since by increasing the load on the soil the cohesive and adhesive forces weaken faster, thus big chunks of burnt tomato puree are released. By increasing the speed, the shear rate increases which enhances both chunk removal and dissolution. The data suggests the increase of chunk removal was higher for speed 200 mm s$^{-1}$ compared to 50 and 100 mm s$^{-1}$. The high standard deviation is expected since number of factors can affect the measurements, for example chunks of tomato puree were still dissolving in water after they were removed from the disc and stayed inside the MTM chamber and small tomato particles can accumulate and change the composition of the samples by the measurement time. Thus, the results for the dissolved mass may not be as accurate as the gravimetric results.

## 4. Conclusion

In present work, cleaning experiments of burnt tomato paste were conducted in a tribometer, the Mini Traction Machine (MTM), to understand the cleaning mechanism of food foulant, and to differentiate the contributions of mechanical force and dissolution.

Indentation measurements show that the mechanical properties of

food foulant change as a function of exposure time to water. The transition of strong cohesion/adhesion to partial adhesion and finally weak cohesion/adhesion was quantitatively identified by the micromanipulation technique. Additionally, it was observed that adhesion was stronger than cohesion for short soaking times but for longer soaking times the opposite was true.

Mechanical properties of food foulant play an important role in cleaning, as demonstrated by the MTM. Two main removal mechanisms were observed in these cleaning experiments, dissolution and removal of chunks of the food foulant. The cleaning rate was steady in most cases and the effects of different parameters were investigated. The different amount of food foulant mass did not affect the cleaning rate under otherwise identical conditions. By increasing applied load or speed the cleaning rate increases and the chunk removal mechanism was boosted, detected by UV–Vis measurements, due to faster weakening of adhesion and cohesion forces.

Tribology results were obtained during this cleaning process, and visual observation helped to explain the behaviour of the friction coefficient graphs. Initially the friction coefficient was high due to the roughness of tomato puree, but it decreased and stabilised as the surface became softer. When areas of the tomato puree disc began to be removed, creating areas of stainless-steel surface, the friction coefficient started increasing and became steady when the tomato puree was completely removed. The MTM provided some wear data, which were analysed to produce cleaning rates, which were similar to the cleaning rates calculated from gravimetric results, thus mass and wear were correlated successfully. The data suggests wear results can be used to calculate cleaning rates, which would be faster in future experiments than the methods using weighing and measurement of dissolved material developed here.

Our results, based on a representative tough soil, suggest that surface removal of food foulant can be approached by tribological principles, which provides a useful method in developing sustainable solutions for food cleaning in the future.

## CRediT authorship contribution statement

**Perrakis Bistis:** Conceptualization, Data curation, Formal analysis, Investigation, Methodology, Validation, Writing – original draft, Writing – review & editing. **Patricia Andreu Cabedo:** Formal analysis, Methodology, Validation. **Serafim Bakalis:** Conceptualization, Methodology, Validation. **Michael Groombridge:** Conceptualization, Methodology, Validation. **Zhenyu Jason Zhang:** Conceptualization, Methodology, Project administration, Supervision, Writing – original draft, Writing – review & editing. **Peter J. Fryer:** Conceptualization, Funding acquisition, Methodology, Project administration, Supervision, Validation, Visualization, Writing – original draft, Writing – review & editing.

## Declaration of competing interest

The authors declare that they have no known competing financial interests or personal relationships that could have appeared to influence the work reported in this paper.

## Data availability

Data will be made available on request.

## Acknowledgments

Authors acknowledge funding received from EPSRC through the Centre for Doctoral Training in Formulation Engineering (grant no. EP/L015153/1), and from Procter and Gamble. ZJZ would like to thank the Royal Academy of Engineering for an Industrial Fellowship (IF2021/100) to work with Procter and Gamble.

## References

Arzate-Vázquez, I., Chanona-Pérez, J., Rodríguez-Castro, G.A., Fuerte-Hernández, A., Méndez-Méndez, J.V., Gutiérrez-López, G.F., 2015. Indentation technique: overview and applications in food science. In: Food Engineering Series. Springer, pp. 81–98. https://doi.org/10.1007/978-3-319-13596-0_6.

Avila-Sierra, A., Huellemeier, H.A., Zhang, Z.J., Heldman, D.R., Fryer, P.J., 2021a. Molecular understanding of fouling induction and removal: effect of the interface temperature on milk deposits. ACS Appl. Mater. Interfaces 13, 35506–35517. https://doi.org/10.1021/acsami.1c09553.

Ávila-Sierra, A., Zhang, Z.J., Fryer, P.J., 2021b. Effect of surface roughness and temperature on stainless steel - whey protein interfacial interactions under pasteurisation conditions. J. Food Eng. 301, 110542 https://doi.org/10.1016/j.jfoodeng.2021.110542.

Basso, M., Simonato, M., Furlanetto, R., De Nardo, L., 2017. Study of chemical environments for washing and descaling of food processing appliances: an insight in commercial cleaning products. J. Ind. Eng. Chem. https://doi.org/10.1016/j.jiec.2017.03.041.

Bhushan, B., 2013. Introduction to tribology. In: Introduction to Tribology, second ed. John Wiley and Sons. https://doi.org/10.1002/9781118403259. Second Edition.

Blau, P.J., 2009. Friction Science and Technology from Concepts to Applications. CRC Press.

Borodich, F.M., Keer, L.M., 2004. Contact problems and depth-sensing nanoindentation for frictionless and frictional boundary conditions. Int. J. Solid Struct. 41, 2479–2499. https://doi.org/10.1016/j.ijsolstr.2003.12.012.

Bunghez, R., Raduly, M.F., Doncea, S.M., Aksahin, I., 2011. Lycopene determination in tomatoes by different spectral techniques (UV-VIS, FTIR and HPLC). Dig. J. Nanomater. Biostruct. 6, 1349–1356.

Cahn, A., Lai, K.-Y., 2006. Liquid Detergents, second ed. Taylor & Francis Group, Santa Barbara. https://doi.org/10.1201/9781420027907.ch1.

Chateau, M.-E., Galet, L., Soudais, Y., Fages, J., 2004. A new test for cleaning efficiency assessment of cleaners for hard surfaces. J. Surfactants Deterg.

Fernández Farrés, I., Norton, I.T., 2015. The influence of co-solutes on tribology of agar fluid gels. Food Hydrocolloids 45, 186–195. https://doi.org/10.1016/j.foodhyd.2014.11.014.

Fischer-Cripps, A.C., 2011. Nanoindentation, Mechanical Engineering Series. Springer New York, New York, NY. https://doi.org/10.1007/978-1-4419-9872-9.

Fryer, P.J., Christian, G.K., Liu, W., 2006. How hygiene happens: physics and chemistry of cleaning. Int. J. Dairy Technol. 59, 76–84. https://doi.org/10.1111/j.1471-0307.2006.00249.x.

Garrec, D.A., Norton, I.T., 2012. The influence of hydrocolloid hydrodynamics on lubrication. Food Hydrocolloids 26, 389–397. https://doi.org/10.1016/j.foodhyd.2011.02.017.

Herrera-Márquez, O., Serrano-Haro, M., Vicaria, J.M., Jurado, E., Fraatz-Leál, A.R., Zhang, Z.J., Fryer, P.J., Avila-Sierra, A., 2020. Cleaning maps: a multi length-scale strategy to approach the cleaning of complex food deposits. J. Clean. Prod. 261, 121254 https://doi.org/10.1016/j.jclepro.2020.121254.

Hertz, H., 1882. Ueber die Berührung fester elastischer Körper. J. Reine Angew. Math. 156–171. https://doi.org/10.1515/crll.1882.92.156, 1882.

Hooper, R.J., Liu, W., Fryer, P.J., Paterson, W.R., Wilson, D.I., Zhang, Z., 2006. Comparative studies of fluid dynamic gauging and a micromanipulation probe for strength measurements. Food Bioprod. Process. 84, 353–358. https://doi.org/10.1205/fbp06038.

Joppa, M., Köhler, H., Kricke, S., Majschak, J.P., Fröhlich, J., Rüdiger, F., 2019. Simulation of jet cleaning: diffusion model for swellable soils. Food Bioprod. Process. 113, 168–176. https://doi.org/10.1016/j.fbp.2018.11.007.

Joppa, M., Köhler, H., Rüdiger, F., Majschak, J.P., Fröhlich, J., 2020. Prediction of cleaning by means of computational fluid dynamics: implication of the pre-wetting of a swellable soil. Heat Tran. Eng. 41, 178–188. https://doi.org/10.1080/01457632.2018.1522096.

Joppa, M., Köhler, H., Rüdiger, F., Majschak, J.P., Fröhlich, J., 2017. Experiments and simulations on the cleaning of a swellable soil in plane channel flow. Heat Tran. Eng. 38, 786–795. https://doi.org/10.1080/01457632.2016.1206420.

Köhler, H., Liebmann, V., Joppa, M., Fröhlich, J., Majschak, J.-P., Rüdiger, F., 2019. On the concept of CFD-based prediction of cleaning for film-like soils. In: Proceedings of 13th International Conference on Heat Exchanger Fouling and Cleaning 2019. Presented at the Heat Exchanger Fouling and Cleaning, p. 8. Warsaw, Poland.

Kurowski, P., Vautrin, C., Genet, P., Hattali, L., Peralta y Fabi, R., Kolb, É., 2018. Mechanical Properties of Drying Plant Roots: Evolution of the Longitudinal Young's Modulus of Chick-Pea Roots with Desiccation Pascal. ArXiv e-prints 1–38.

Liu, W., Christian, G.K., Zhang, Z., Fryer, P.J., 2002. Development and use of a micromanipulation technique for measuring the force required to disrupt and remove fouling deposits. Food Bioprod. Process. 80, 286–291. https://doi.org/10.1205/096030802321154790.

Liu, W., Fryer, P.J., Zhang, Z., Zhao, Q., Liu, Y., 2006a. Identification of cohesive and adhesive effects in the cleaning of food fouling deposits. Innovat. Food Sci. Emerg. Technol. 7, 263–269. https://doi.org/10.1016/j.ifset.2006.02.006.

Liu, W., Zhang, Z., Fryer, P.J., 2006b. Identification and modelling of different removal modes in the cleaning of a model food deposit. Chem. Eng. Sci. 61, 7528–7534. https://doi.org/10.1016/j.ces.2006.08.045.

Lütkenhaus, D., Cao, H., Dearn, K.D., Bakalis, S., 2016. The tribology of cleaning processes. Tribol. Online 11, 298–307. https://doi.org/10.2474/trol.11.298.

Maillard, L.C., 1912. Action des acides amines sur les sucres; formation des melanoidines par voie methodique. Comptes R. Acad. Sci.(Paris) 154, 66–68.

Mercadé-Prieto, R., Bakalis, S., 2014. Methodological study on the removal of solid oil and fat stains from cotton fabrics using abrasion. Textil. Res. J. 84, 52–65. https://doi.org/10.1177/0040517513490059.

Mercadé-Prieto, R., Bakalis, S., 2013. Washing simulator rig to study the effect of abrasion on the removal of soils from fabrics. Tribol. Lett. 52, 175–183. https://doi.org/10.1007/s11249-013-0236-5.

MTM, 2017. (Mini Traction Machine) | Products. PCS Instruments [WWW Document]. https://pcs-instruments.com/product/mtm-mini-traction-machine/. accessed 4.18.18.

Oliver, W.C., Pharr, G.M., 2004. Measurement of Hardness and Elastic Modulus by Instrumented Indentation: Advances in Understanding and Refinements to Methodology.

Oliver, W.C., Pharr, G.M., 1992. An Improved Technique for Determining Hardness and Elastic Modulus Using Load and Displacement Sensing Indentation Experiments.

Otto, C., Zahn, S., Hauschild, M., Babick, F., Rohm, H., 2016. Comparative cleaning tests with modified protein and starch residues. J. Food Eng. 178, 145–150. https://doi.org/10.1016/j.jfoodeng.2016.01.015.

Pérez-Mohedano, R., Letzelter, N., Bakalis, S., 2017. Integrated model for the prediction of cleaning profiles inside an automatic dishwasher. J. Food Eng. 196, 101–112. https://doi.org/10.1016/j.jfoodeng.2016.09.031.

Prakash, S., 2017. From rheology to tribology: applications of tribology in studying food oral processing and texture perception. In: Advances in Food Rheology and its Applications. Elsevier Inc., pp. 65–86. https://doi.org/10.1016/B978-0-08-100431-9.00004-8

Sinha, A., Bhargav, A., 2020. Young's modulus estimation in food samples: effect of experimental parameters. Mec. Ind. 21 https://doi.org/10.1051/meca/2020025.

Taylor, B.L., Mills, T.B., 2020. Using a three-ball-on-plate configuration for soft tribology applications. J. Food Eng. 274, 109838 https://doi.org/10.1016/j.jfoodeng.2019.109838.

Uner, A., Yilmaz, F., 2015. Efficiency of laundry polymers containing liquid detergents for hard surface cleaning. J. Surfactants Deterg. 18, 213–224. https://doi.org/10.1007/s11743-014-1634-x.

Vicaria, J.M., Jurado-Alameda, E., Herrera-Márquez, O., Olivares-Arias, V., Ávila-Sierra, A., 2017. Analysis of different protocols for the cleaning of corn starch adhering to stainless steel. J. Clean. Prod. 168, 87–96. https://doi.org/10.1016/j.jclepro.2017.08.232.